Journal of Ceramic Processing Research. Vol. 10, No. 4, pp. 521~525 (2009)

J O U R N A L O F
Ceramic Processing Research

Lateral assembly of millimetre-long silicon nanowires for multiple device integration

Yong Bum Pyun, Dong Hyun Lee, Jae Seok Yi, Yong-Jae Kim, Jae-il Jang and Won Il Park*
Division of Materials Science and Engineering, Hanyang University, Seoul 133-791

Ultralong one-dimensional nanostructures can serve as unique building blocks that interlink nanometre-scale materials with those in the real macroscopic world. Here we report on the lateral assembly of millimetre-long silicon (Si) nanowires (MML-SiNWs) synthesized through a metal-catalyzed vapor-liquid-liquid method by a soft-contact-printing (SCP) process. In our approach, the pressure and shear force between NWs and the substrate surface were systematically varied by the gliding angle and weight of the receiver substrate, which can assemble MML-SiNWs into parallel arrays with a controlled density. These MML-SiNW building blocks have been configured as multiple device arrays by wiring hundreds of electrodes onto a single wire by conventional photolithography. Transport measurements demonstrated uniform electrical properties along the millimetre-length of the SiNWs with a high-channel conductance of ~5 μS.

Key words: Millimeter-long silicon nanowires, Assembly, Contact printing, Nanoelectronics.

Introduction

Single-crystalline nanostructures, such as semiconducting nanowires (NWs) [1, 2], have been widely studied as they are promising elements for future nanoelectronics [3] and photonics [4,5] due to their unique characteristics and intrinsically miniature dimensions. The creation of more sophisticated electronic circuits [6] and multiplexing biosensors [7] is enabled by the interconnection of multiple NW devices. The development of these integrated electronic systems, meanwhile, requires a technique that can enable the efficient assembly of NWs into specific array structures with high reproducibility and control [8-12]. The use of ultralong one-dimensional (1D) nanostructures with uniform electronic properties and the integration of multiple devices directly onto them would be a promising alternative to ensure a more reliable and uniform device performance, and to expand their applications into the complex electronic circuit level. In particular, objects whose lengths are beyond the macroscopic scale and reach the size of an integrated system have the potential to be fully used in functional nanosystems by the direct integration of a large number of device elements into a single wire. Recently, millimetre-long silicon nanowires (MML-SiNWs) exhibiting a high degree of electrical uniformity along the entire length of wires were successfully synthesized by introducing disilane (Si_2H_6) as a chemical vapor source in a metal-catalyzed vapor-liquid-liquid process [13]. However, these SiNWs are easily bent, tend to get entangled, and broken into small pieces during the transfer and assembly, and therefore it is important to find a strategy to align and extend the MML-SiNWs with a controlled density for fabricating integrated nanoelectronic systems.

Here we describe a 'soft-contact-printing' (SCP) method that enables the lateral assembly of MML-SiNWs on receiver substrates for multiple device integration. The key feature of this strategy, in comparison with a reported shear contact printing process [11, 14], is that the pressure and shear force between the NWs and substrate surface were systematically adjusted, which can minimize the breakage of the MML-SiNWs and thereby enable the control of the density, alignment, and length of the printed MML-SiNWs on the target substrate.

Experimental

Synthesis of MML-SiNWs

MML-SiNWs were synthesized by CVD using well-dispersed gold nanoclusters as catalysts, H_2 as the carrier gas (5-30 standard cubic centimetres per minute, sccm) and Si_2H_6 (1-5 sccm) as the reactant source (Fig. 1(a)) [13]. During synthesis, the reactor pressure and temperature were kept at 1.33 kPa and 400 ºC, respectively. For *p*-type doping, 100 p.p.m. B_2H_6 was employed as the doping source with a Si_2H_6/B_2H_6 feeding ratio of 10^5–10^6 : 1 (Si/B = 10^5 – 10^6 : 1).

Soft-contact-printing of MML-SiNWs

Fig. 1(b) schematically illustrates the SCP process of transferring the MML-SiNWs from the growth substrate (1 cm × 5 cm) onto the receiver substrate (1 cm × 1 cm). First, the SiNW growth substrate was fixed on the plate

*Corresponding author:
Tel : +82-2-2220-0504
Fax: +82-2-2220-0389
E-mail: wipark@hanyang.ac.kr

www.kci.go.kr

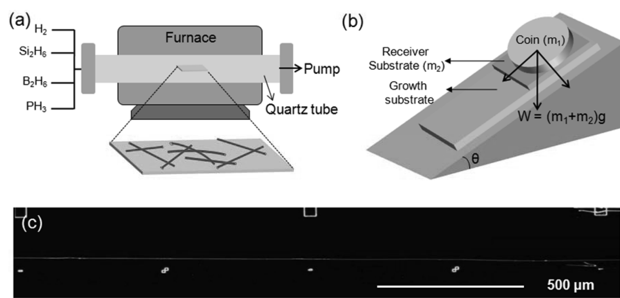

Fig. 1. Synthesis and assembly of MML-SiNWs, (a) Schematic of the NW growth apparatus, (b) Schematic illustration of the SCP process used for printing of MML-SiNWs, (c) Dark-field optical image of MML-SiNWs printed on the receiver substrate, The MML-SiNW is spread out and well aligned along the printing direction.

with an angle of inclination (θ) of 30-60°. Second, the receiver substrate was placed opposite the growth substrate in such a way that the NWs on the growth substrate were in contact with the receiver substrate surface. Then, the receiver substrate slid down the slope on the growth substrate by gravitation. During the substrate's glide of the substrate the shear force enables the transfer of the NWs from the growth substrate to the receiver substrate, and aligns them along the printing direction (Fig. 1(c)). The net weight of the receiver substrate (W) was systematically varied in the range of 0.12-7.5 gf by attaching various masses of coins (m_1) to the backside of the substrate (m_2). Together with the gliding angle (θ), the W determines the pressure and shear force between NWs and the substrate surface.

Fabrication of SiNW devices and electrical characterization

SiNW devices were fabricated on degenerately doped (resistivity < 0.005 Ω·cm) silicon (100) substrates coated with 1-μm-thick layer of SiO_2. Multiple electrodes to the MML-SiNWs were defined by photolithography, followed by the evaporation of 70-nm-thick Ni contacts. Rapid thermal annealing was carried out at 280 °C for 1 minute in a forming gas (10% H_2 in N_2) to form low-resistance NiSi contacts at the interface between the Ni and SiNWs [7]. Current-voltage (I-V) characteristics of the SiNW devices were measured at room temperature in ambient air using a semiconductor parameter analyzer (4156C).

Results and Discussion

Fig. 2(a) shows the general morphology of as-grown MML-SiNWs using Si_2H_6 reactant gas at 400 °C for 30 minutes. Quantitative analysis showed that average length and standard deviation values are ~980 nm and 360 nm,

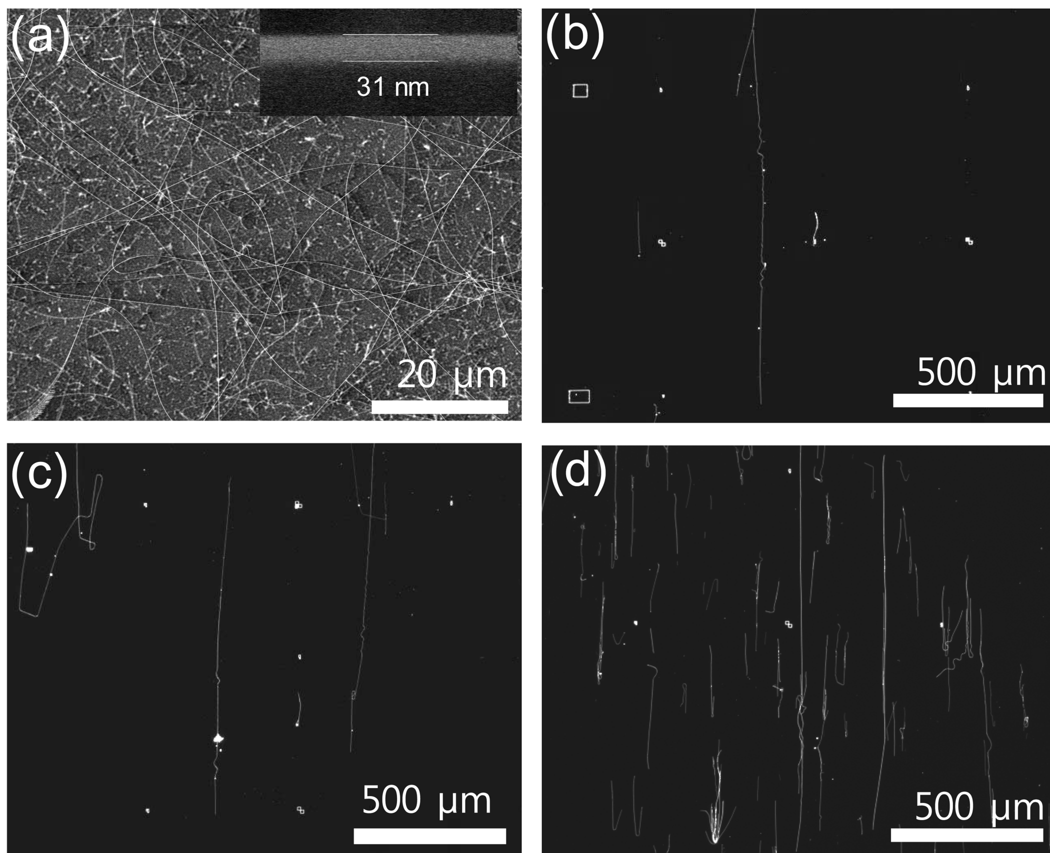

Fig. 2. (a) SEM image of the as-grown MML-SiNWs. Inset: enlarged SEM image of the MML-SiNW with a diameter of 31 nm. (b)-(d) Dark-field optical images of the MML-SiNWs transferred to the target substrates with various printing conditions: (b) W = 0.12 gf, θ = 30°, (c) W = 3.1 gf, θ = 30°, (d) W = 7.5 gf, θ = 30°.

www.kci.go.kr

respectively, whereas their diameter is as small as ~20-30 nm, comparable to the size of the Au nanoclusters (Fig. 2(a), inset).

A soft-contact-printing method was used to transfer the MML-SiNWs to the receiver substrates. Representative optical microscopy (OM) images of the MML-SiNWs transferred to the substrates with various printing conditions show several important features (Figs. 2(b)-(d)). First, the SiNWs are spread out and aligned along the printing direction, and the alignment readily extends over the centimetre scale. Analysis of the transferred SiNWs shows that more than 70-80% of the NWs are aligned within $\pm 5^{o}$ with respect to the gliding direction of the receiver substrate. It is noted that the NW alignment can be explained by the shear force being between the NWs and substrates [8, 11], and thus increasing the gliding angle can induce larger shear forces and hence improve the degree of alignment. Second, the coverage of transferred MML-SiNWs increases with the weight of the receiver substrate, W. To quantitatively analyze the coverage of transferred MML-SiNWs, the W was systematically varied in the range of 0.12-7.5 gf while maintaining the gliding angle at 30°, and the results are summarized in Fig. 3(a). In case of $W = 7.5$ gf, the mean value of the total printed NW length per unit area was about 5.2 mm^{-1}, which is roughly 10 times larger than that of the bare receiver substrate with no coin ($W = 0.12$ gf).

In addition, the average length of the individual SiNWs printed on the receiver substrate decreases with increasing W (Fig. 3(b)). When unlubricated, solid surfaces slide over each other, the magnitude of the frictional force F is given by $F = \mu N$, where μ is the coefficient of kinetic friction and N is the magnitude of the surface normal force that is defined as $N = W{\cdot}\cos\theta$ in the SCP process. Therefore, in case of $W = 7.5$ gf, a large frictional force enhances the undesirable breakage of NWs during the sliding of the receiver substrates (Fig. 2(d)), resulting in a decrease of the mean NW length to ~230 μm. To increase the average length of the printed NWs, the frictional force may be minimized by reducing the W. By using a bare substrate without coins ($W = 0.12$ gf), we can achieve the longest NWs with a mean length of ~650 μm, approaching the as-grown NW length of ~980 μm. It should be noted that, as Fan *et al.* have pointed out, using a lubricant during the contact printing process can further minimize the breakage of NWs by reducing the friction force [14].

The well-aligned MML-SiNWs, as compared with micrometre-long NWs, could serve as unique building blocks for integrating 1D device arrays onto single wires [13]. In particular, as shown in Fig. 1(c), the MML-SiNWs are clearly observed in the optical microscope, and therefore, these materials offer great potential as unique building blocks for fabricating complex electronic systems through the use of conventional semiconductor processing. To demonstrate this concept, we have made multiple devices by photolithography instead of electron

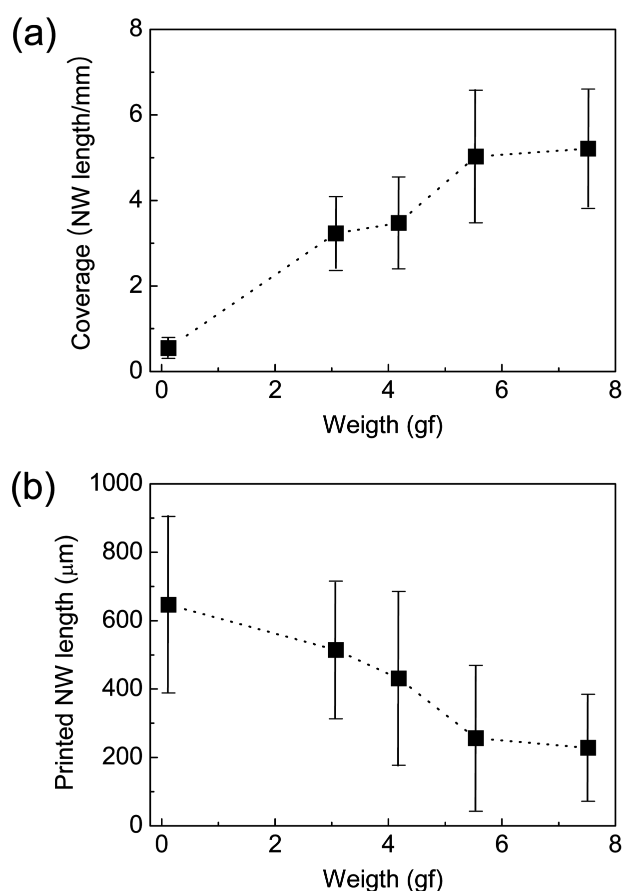

Fig. 3. (a) Coverage of the printed MML-SiNWs depending on the weight of the receiver substrate, W. (b) Average length of the printed MML-SiNWs depending on *W*.

beam lithography [3, 4, 6, 8]. Fig. 4 schematically describes the device fabrication process. Using the SCP process, as-grown MML-SiNWs were deposited onto SiO_2/Si substrate (Fig. 4(a)). Then, the outer contact pads and interconnects were defined by photolithography, followed by the sequential deposition of Cr and Au (Fig. 4(b)). In this step, we have used a negative photoresist (SU8-2002, Micro-Chem) instead of the positive photoresist, since the photomask designed for a negative photoresist is transparent on the exterior of the pads and interconnects, thus enabling the alignment of the photomask with respect to the printed NW using an optical microscope. Finally, the contact electrodes and inner interconnects were defined by photolithography using a positive photoresist (S1805, Shipley), and then 70-nm-thick Ni was deposited for contacts.

Figs. 5(a) and (b) show the central region of the device array, where hundreds of electrode pairs are formed over a 1.3-mm-long MML-SiNW. An enlarged SEM image of the device corresponding to the rectangle in Fig. 5(b) shows that electrode pairs separated by 3 μm were formed on ~32-nm-thick SiNW. To assess the electrical properties of the NW devices, I-V characteristic curves were investigated in the regions I, II, and III of the device

www.kci.go.kr

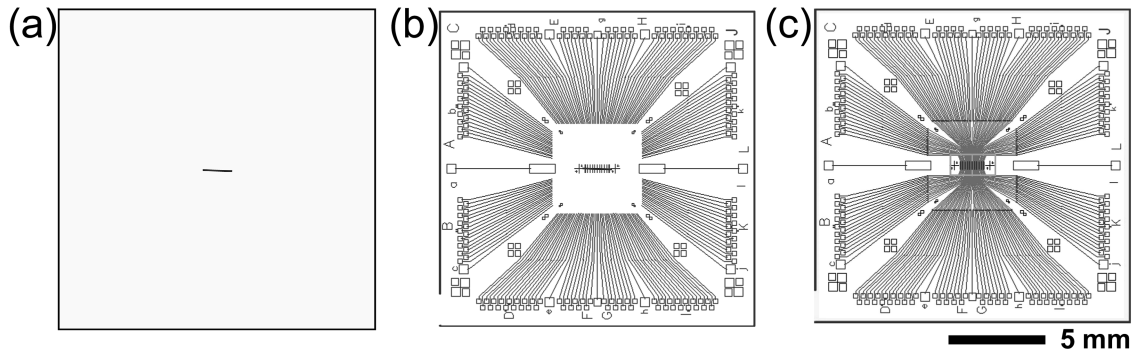

Fig. 4. Schematic illustration of the key fabrication steps of the 1D device array onto the MML-SiNWs by conventional semiconductor processing, (a) Deposition of well-isolated and aligned MML-SiNWs by the SCP process, (b) Fabrication of the outer contact pads and interconnects. Using an optical microscope, the photomask was aligned with respect to the printed NWs, (c) Fabrication of the contact electrodes and inner interconnects.

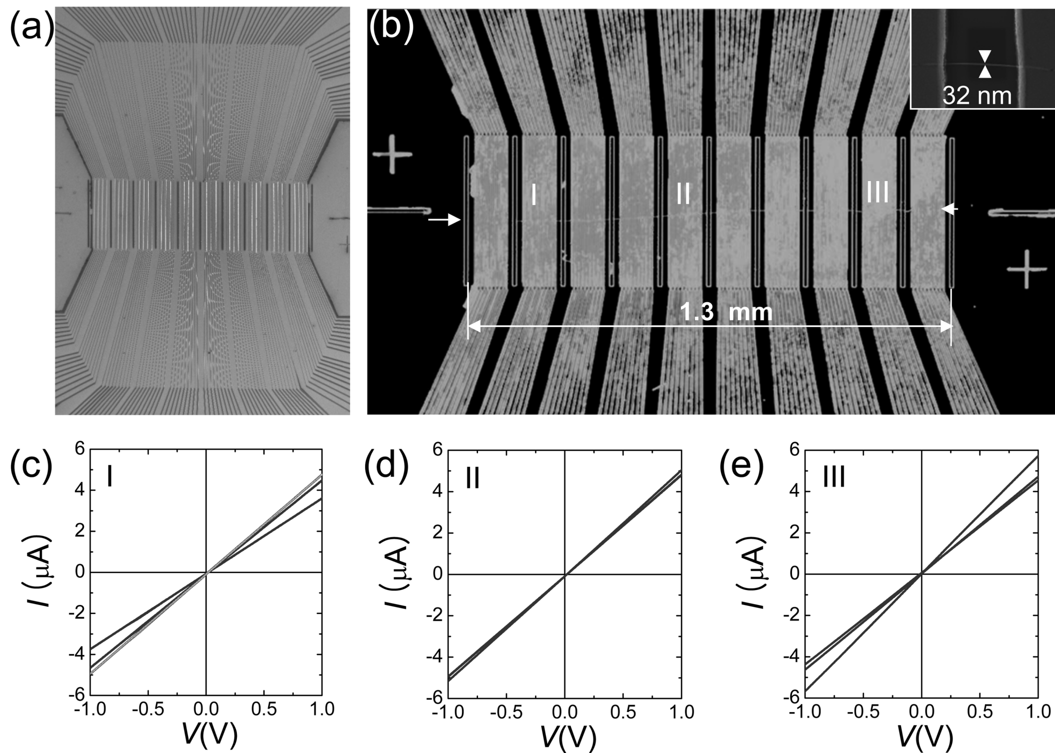

Fig. 5. (a) Low magnification SEM images of a multiple electrode array fabricated on a MML-SiNWs, (b) Dark-field optical image of multiple devices corresponding to the rectangle in (a) shows that hundreds of electrode pairs are formed over a 1.3 mm-long SiNW. Inset, a high-magnification SEM image shows that ~32-nm-thick SiNW is connected with the electrode pairs separated by 3 μm. (c)-(e) I-V curves collected in regions I, II, and III of the single-NW multiple devices in (b).

array and are plotted in Figs. 5(c)-(e). Most of the devices exhibited linear and symmetric I-V characteristic curves, representing the formation of low-resistance Ohmic contacts between the SiNW and the Ti metal layer. In addition, the current levels along the millimetre-long wires are relatively uniform, indicating the homogeneous electrical properties of SiNWs. The average NW channel conductance is as high as ~5.1 μS with a standard deviation of 0.4 μS. Considering the mean diameter of 32 nm, we obtained a NW conductivity value of ~190 $(\text{Ohm-cm})^{-1}$, comparable to that of reported individual SiNW devices, ~100-400 $(\text{Ohm-cm})^{-1}$ [15].

Conclusions

We have developed a simple and general approach for the lateral assembly of MML-SiNWs into parallel arrays, where the shear force between substrates and NWs was exploited to spread out and align the NWs along the printing direction. In particular the pressure and shear force between the NWs and substrate surface were systematically varied to control the average length and coverage of printed NWs. In addition, a 1D device array fabricated by wiring hundreds of electrodes onto a single MML-SiNW using conventional photolithography

www.kci.go.kr

demonstrates the huge potential of bringing nanometre-scale objects into the macroscopic world.

Acknowledgements

This work was supported by the Korea Science and Engineering Foundation (KOSEF) grant funded by the Korea government(MEST) (No. KOSEF R01-E008-000-20778-0).

References

1. C.M. Lieber, Sci. Am. 285 (2001) 50-56.
2. G.-C. Yi, C. Wang, and W.I. Park, Semicond. Sci. Technol. 20[4] (2005) S22-S34.
3. Y. Cui, and C.M. Lieber, Science 291 (2001) 851-853.
4. X. Duan, Y. Huang, Y. Cui, J. Wang and C.M. Lieber, Nature 409[6816] (2001) 66-68.
5. W.I. Park and G.-C. Yi, Adv. Mater. 16[1] (2004) 87-90.
6. W.I. Park, J.S. Kim, G.-C. Yi and H.-J. Lee, Adv. Mater. 17[11] (2005) 1393-1397.
7. F. Patolsky, G. Zheng and C.M. Lieber, Nat. Protocols 1[3] (2006) 1711-1724.
8. Y. Huang, X. Duan, Q. Wei and C.M. Lieber, Science 291 (2001) 630-633.
9. S. Jin, D. Whang, M.C. McAlpine, R.S. Friedman, Y. Wu and C.M. Lieber, Nano Lett. 4[5] (2004) 915-919.
10. P. Yang, Nature 425[6955] (2003) 243-244.
11. A. Javey, S. Nam, R.S. Friedman, H. Yan and C.M. Lieber, Nano Lett. 7[3] (2007) 773-777.
12. Y.J. Hong, S.J. An, H.S. Jung, C.-H. Lee and G.-C. Yi, Adv. Mater. 19[24] (2007) 4416-4419.
13. W.I. Park, G. Zheng, X. Jiang, B. Tian and C.M. Lieber, Nano Lett. 8[9] (2008) 3004-3009.
14. Z. Fan, J.C. Ho, Z.A. Jacobson, R. Yerushalmi, R.L. Alley, H. Razavi and A. Javey, Nano Lett. 8[1] (2008) 20-25.
15. Y. Cui, Z. Zhong, D. Wang, W.U. Wang and C.M. Lieber, Nano Lett. 3[2] (2003) 149-152.

www.kci.go.kr